Wireless Pers Commun (2013) 71:1511–1521
DOI 10.1007/s11277-012-0889-7

Analysis of the Effect of Ground Plane Size on the Performance of a Probe-fed Cavity Resonator Microstrip Antenna

Kumud Ranjan Jha · G. Singh

Published online: 25 October 2012

Abstract In this paper, a probe-fed rectangular microstrip patch antenna with partially reflective superstrate at terahertz frequency (600 GHz) has been analyzed and simulated. The analysis of the partially reflective surface shows the highly reflective property of the surface over the wideband of the frequencies. The analysis of a specific configuration (rectangular patch) of partially reflective surface predicts the directivity of antenna to be the order of 24 dBi and subsequently it has been validated with the simulation. The proposed antenna has been simulated by using commercially available CST Microwave Studio simulator based on finite integral technique. Next to this, the application scenario of this kind of the antenna in the terahertz regime of the electromagnetic spectrum has been discussed and it has been obtained that this antenna is capable to establish 9 m long communication link.

Keywords Probe-fed-microstrip antenna · Terahertz spectrum · Directivity · Frequency-selective-surface

1 Introduction

Demand is increasing for higher data rate in the wireless communications in order to keep up with the remarkable speed-up of fiber-optic networks. One of the most direct and easiest ways to achieve the higher data rate is to use carrier waves whose frequencies lies into the terahertz regime of the electromagnetic spectrum [1]. Recently, the communication systems in the millimeter wave (60 GHz) have been developed. In addition to this, the terahertz wireless communication system at 100 and 300 GHz is also being developed [2,3]. When the operating

K. R. Jha
School of Electronics and Communication Engineering, Shri Mata Vaishno Devi University, Katra, Jammu and Kashmir, India

G. Singh (✉)
Department of Electronics and Communication Engineering, Jaypee University of Information Technology, Solan 173234, India
e-mail: drghanshyam.singh@yahoo.com

frequency of the system is increased, the overall performance of the system is deteriorated due to the high atmospheric attenuation rate of the electromagnetic signal. Fortunately, there are a number of low atmospheric windows in the lower terahertz frequency regime spectrum where the successful short distance wireless communication can be established [4]. However, it is necessary to increase the directivity of the antenna to combat the path-loss and to increase the transmission and reception range of the wireless communication system. A highly directive antenna can be realized by using the thick substrate material or the substrate lenses [5,6]. However, there is the problem of energy trapping within the substrate material.

The next class of the antenna at terahertz frequency is designed as the photoconductive antennas [7]. However, the low gain and poor impedance matching is the inherent drawback of this kind of the antennas. Moreover, this class of the antenna needs an integration of source and radiator. On this way the practical application of these antennas in the communication systems is restricted. Apart from this, several antenna designs at 600 GHz have been presented by various researchers [8–14]. Some of them show the improvement in the directivity but still lacks to meet the requirement of high directivity at terahertz frequency. In the microwave frequency regime, the superstrate antennas with the frequency selective surfaces (FSS) are frequently used to enhance the directivity and promising results have been obtained [15–19]. However, there are enough evidences to support the propagation of the terahertz electromagnetic wave over the metallic-clad low dielectric permittivity substrate materials [20,21]. On this way, it is well understood that the highly directive microstrip antenna with the help of low-dielectric permittivity copper-clad can also be designed at the terahertz frequency.

This manuscript is aimed to the analysis and design of a highly directive terahertz microstrip antenna using the frequency selective surfaces and its application in the terahertz wireless communication. The organization of the paper is as follows. The Sect. 2 of this manuscript is concerns with the analysis of frequency selective method. The theoretical investigation of the directivity of the cavity resonant antenna (CRA) with the partially reflective surface is presented in the Sect. 3. The numerical analysis of the antenna by using CST Microwave Studio is presented in the Sect. 4. The scaled down model of the antenna at 300 GHz and its application in the terahertz wireless communication has been discussed in the Sect. 5. Finally, Sect. 6 concludes the work.

2 Analysis of Frequency Selective Surface

A rectangular frequency selective surface is shown in Fig. 1. The capacitive type frequency selective surface is made with the copper ($\sigma = 5.8 \times 10^7$ S/m) patch of length, width and thickness equal to 152, 110 and 20 μm, respectively. The dielectric support to the patch

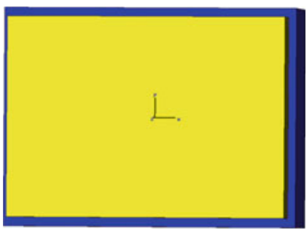

Fig. 1 Unit-cell of the frequency selective surfaces

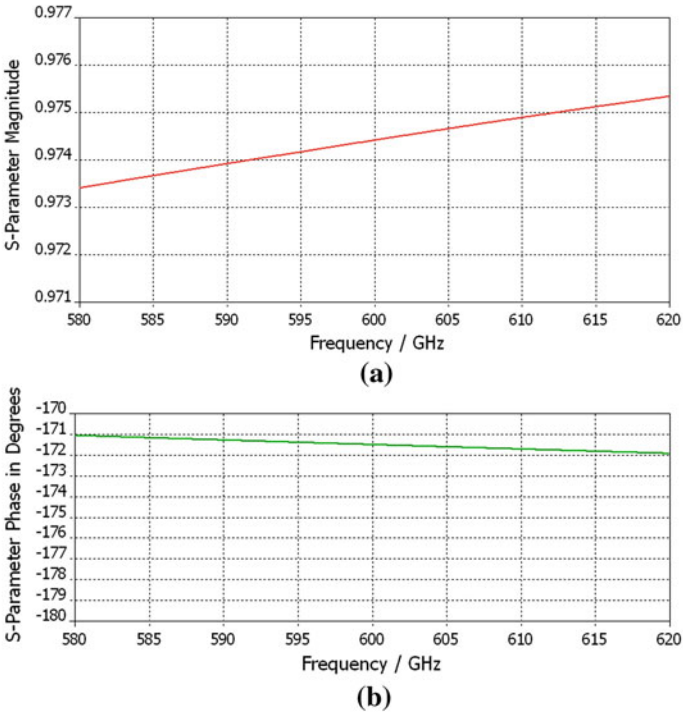

Fig. 2 Frequency response of the frequency selective surface (**a**) magnitude and (**b**) phase angle

is PTFE material having relative dielectric permittivity and loss tangent 2.08 and 0.0004, respectively. The length, width and the thickness of the support are 160, 120 and 50 μm, respectively. When this surface is excited by the normal incident wave ($\theta = 0°$) with the electric field aligned along the length of the rectangular surface, it shows the high reflective property. This property of the surface has been obtained by simulating the structure in the transient solver of the CST Microwave Studio. The excitation procedure of the frequency selective surface unit-cell is discussed in detail in [22]. However, we are only interested in the reflection magnitude and phase of the unit-cell, therefore transmission property of the frequency selective surface unit-cell is not discussed in the present manuscript.

The amplitude and phase of the reflection coefficient at 580–620 GHz frequency regime of the spectrum is shown in Fig. 2(a),(b), respectively. From Fig. 2(a), it is revealed that the magnitude of the reflection coefficient $|S_{11}| > 0.97$ over the simulated frequency range, which predicts that the highly directive antenna can be designed with the help of this frequency selective surface over the wide frequency range. It also indicates the potential advantage of the capacitive type of frequency selective surface in which the highly reflective property can be obtained over the wide range of the frequency [23].

3 Resonance Estimation Using Ray-Tracing

At any operating frequency f, the ray-tracing technique is used to predict the height of the superstrate above the ground plane. The height of the superstrate above the ground plane is expressed by the expression as given in [24].

$$h = \frac{N\lambda}{2} + \left(\left(\phi_g + \phi_{FSS}\right)/\pi\right)\frac{\lambda}{4} \text{ for} N = 1, 2, 3 \ldots . \quad (1)$$

In Eq. (1), h, N, λ, ϕ_g, and ϕ_{FSS} are the height of superstrate above the ground plane, an integer number, wavelength in free-space, reflection phase angle of the ground plane and reflection phase angle of the superstrate unit-cell, respectively. The value of ϕ_{FSS} is obtained from Fig. 2(b) and it is equal to $-171.5°$ at 600 GHz. The value of ϕ_g is obtained by using the expression:

$$\phi_g = \pi - 2\tan^{-1}(Z_d \tan(\beta d)/Z_0) \quad (2)$$

where Z_d and Z_0 are the characteristics impedance of the substrate dielectric and the air, respectively, β is the dielectric phase constant and d is the substrate thickness. By using the above formula as stated in Eq. (2), the value of ϕ_g for the above-mentioned substrate material at 600 GHz is 96.99°. On this way, the value of h is equal to 200 μm to resonate the cavity at 600 GHz and the bore-sight directivity of the cavity with respect to the primary source is obtained by using the following expression [25,26].

$$D = \frac{1 + |\Gamma_{FSS}(f, \theta = 0°)|}{1 - |\Gamma_{FSS}(f, \theta = 0°)|} \quad (3)$$

From Fig. 2(a), it is revealed that the value of $|\Gamma_{FSS}(f, \theta = 0°)|$ is equal to 0.97 and relative directivity of the cavity is 18 dBi. Therefore, when a primary source of the directivity 6–7 dBi (such as microstrip antenna) is placed inside the cavity, the total directivity must increase to 24–25 dBi. However, it is important to mention here that the predicted directivity on this way is achievable only with the semi-infinite ground plane and semi-infinite array of the frequency selective surface.

4 Numerical Simulation

For the clarity of the vision, the wire frame view of two probe-fed microstrip patch antennas are shown in Figs. 3 and 4. The front view of the frequency selective surfaces array is shown in Fig. 5. In the wire-frame view of the structure, black and blue boundaries indicate the copper and PTFE material, respectively. The length (L), width (W) and the thickness of the radiating patch are 152, 110 and 20 μm, respectively. In other words, its geometrical parameters are same as the geometrical parameters of the frequency selective surfaces unit-cell. The patch is followed the PTFE substrate ($\varepsilon_r = 2.08$, tan δ = 0.0004) of length, width and thickness

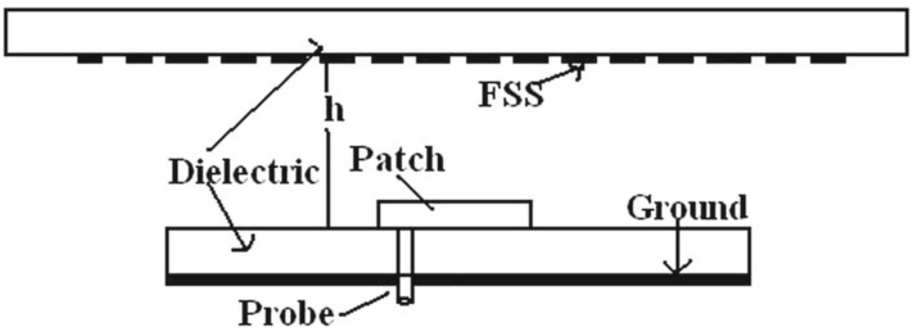

Fig. 3 The frequency selective surfaces superstrate antenna with the reduced ground plane size

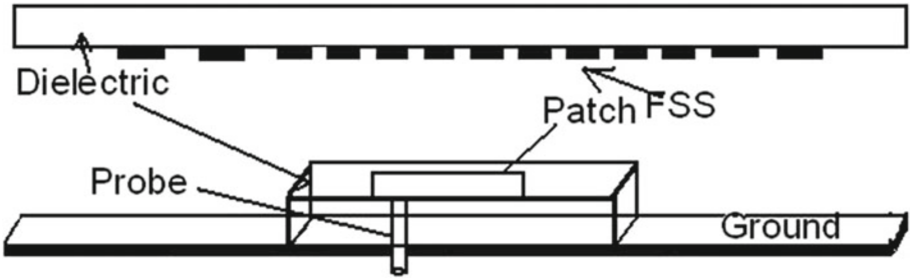

Fig. 4 The frequency selective surfaces superstrate antenna with the extended ground plane size

Fig. 5 Front view of the frequency selective surfaces superstrate antenna

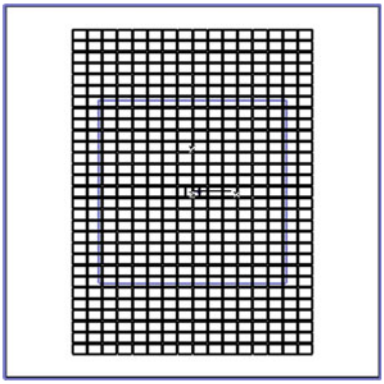

equal to 2,000, 2,000 and 50 μm, respectively. The substrate is followed by a copper ground plane whose dimensions are same as the substrate dimensions in the case of the antenna as shown in Fig. 3. However, to analyze the effect of the size of the ground plane on the electrical performance of the antenna, the length and width of the ground plane of the antenna as shown in Fig. 4 has been increased to 4,000 μm. The patch is excited by a copper wire of radius 5 μm. The feed point is located at $x_0 = 70\mu m$ where $x_0$is the distance of feed point from the centre of the patch on the x-axis. The simple geometry of the patch antennas as shown in Figs. 3 and 4 is loaded by the frequency selective surfaces superstrate array having 16×29 cells along x- and y-axis, respectively. These frequency selective surface cells are supported by the same dielectric material as of the substrate with the same thickness. The height of the frequency selective surface array above the substrate is 205 μm which is in the close agreement to the height predicted in Sect. 3. To predict the correct height of the superstrate above the antenna, several simulations have been run but to reduce the manuscript length they are not shown here.

When the antenna as shown in Fig. 3 is simulated by using CST Microwave Studio Transient solver, it does not provide the expected directivity. Due to the reduced ground plane size in comparison to the frequency selective surfaces array size, the reflected electromagnetic wave by this array is not confined and it is scattered in the surrounding environment. On this way, the perfect collimation of the field in the intended direction does not take place. The scattering phenomenon in this case can be seen in its radiation pattern which is shown in Fig. 6. Due to the scattering of the electromagnetic wave, the antenna also shows the poor impedance matching at the port and it is shown in Fig. 7. On this way, it is emphasized that

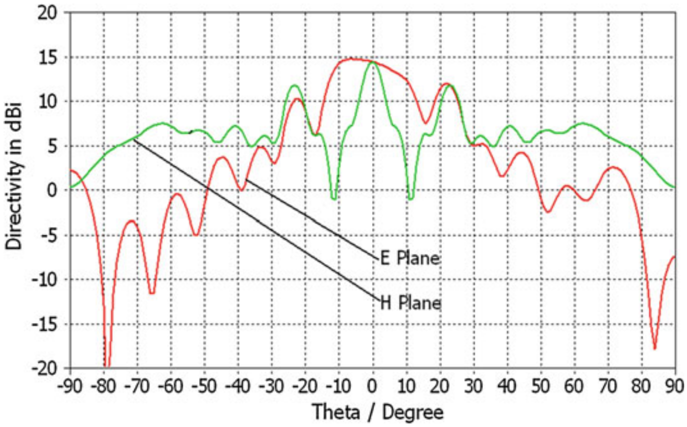

Fig. 6 Radiation pattern of the antenna shown in Fig. 3 at 600 GHz

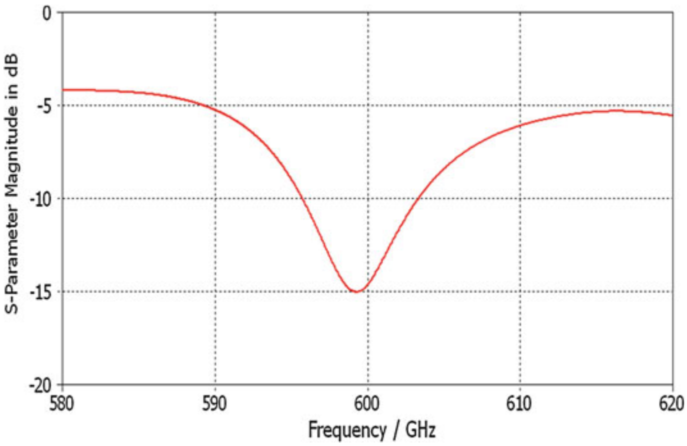

Fig. 7 S_{11} (dB) parameter of the antenna proposed in Fig. 3

the ground plane size must be able to cover the entire the frequency selective surfaces cells for the perfect collimation of the wave.

From Fig. 6, the scattering of the wave in E- plane is clearly visible for the antenna presented in Fig. 3. The simulated directivity and bandwidth of the antenna is about 15.5 dBi and 7.0 GHz, respectively. In spite of the larger superstrate size, the directivity has reduced significantly in the case of the antenna structure presented in Fig. 3.

The directivity of this antenna can only be improved by increasing the ground plane size. Here it is clearly revealed that the ground plane size must be equal to or greater than the size of frequency selective surfaces array. In order to meet this requirement, the size of the ground plane (copper plate) has been increased from $2000 \times 2000 \mu m^2$ to $4000 \times 4000 \mu m^2$ as shown in Fig. 4. In this situation, the directivity of the antenna has increased to 24.67 dBi. Its S_{11} parameter (in dB) and radiation pattern at the resonance frequency are shown in Figs. 8 and 9, respectively. From Fig. 8, it is seen that the resonance frequency of the antenna is decreased with the increase in the size of the ground plane. The reduction in the resonance frequency is mainly due to the change in the dielectric permittivity of the medium above

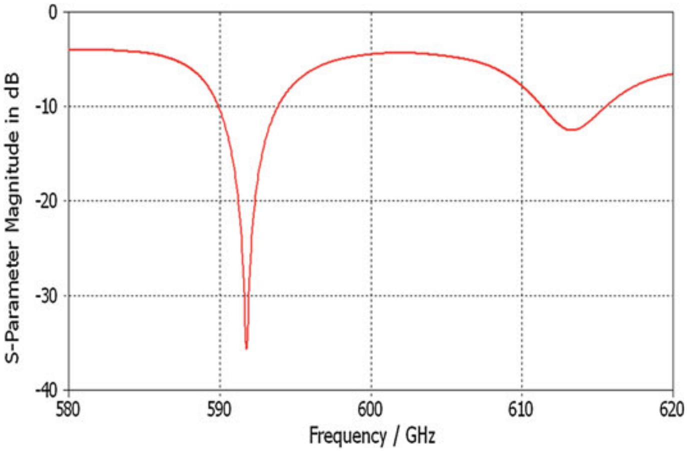

Fig. 8 S_{11} (dB) parameter of the proposed antenna in Fig. 4

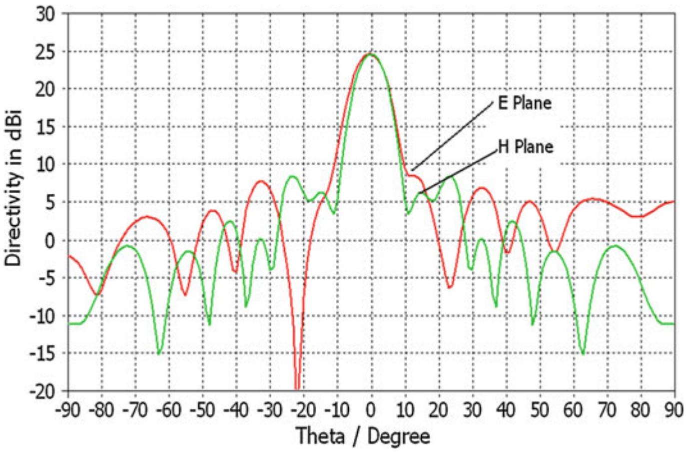

Fig. 9 Radiation pattern of the antenna at 592 GHz

the radiating patch and it is in agreement to the statement made in [23]. The bandwidth of the antenna is reduced to about 3 GHz at 592 GHz resonance frequency. However, the directivity is significantly increased to 24.67 dBi as shown in Fig. 9. Apart from the directivity enhancement, the beam shape is also improved in both planes. The result presented in Fig. 9 is in the close agreement to the predicted directivity in Sect. 3. Therefore, it is concluded that the ray-tracing method can only be satisfied by the semi-infinite ground plane and frequency selective surfaces array size.

It is interesting to note that the capacitive patch has highly reflective property over the wide range of the frequency as discussed in Sect. 2 which indicates that high directivity is achievable in the wide frequency range. It is confirmed from the simulated directivity pattern as presented in Fig. 10 where the minimum directivity is 16 dBi.

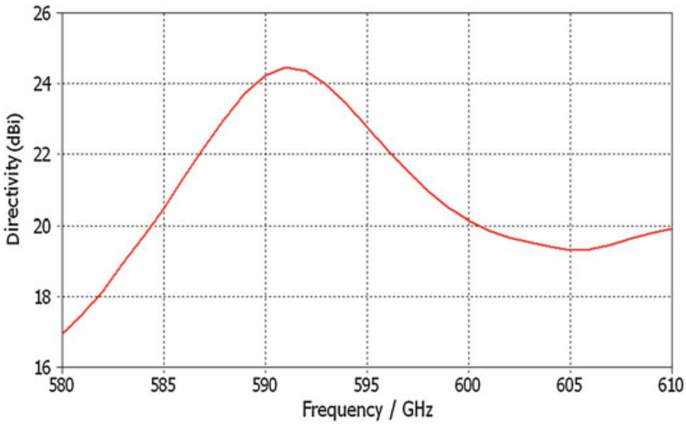

Fig. 10 Directivity pattern of the proposed antenna over a wide frequency range

5 Scale Down Model of the Antenna

Presently, the research in the field of the Terahertz communication is focused around 300 GHz due to the low atmospheric absorption of the electromagnetic wave [3,27] in this region. For the transmission of the wave at this carrier frequency over 10 m, there is the need of 31 dBi gain antenna [27] for the line-of-sight (LOS) communication. Here to demonstrate the practical application of the CRA antenna at this frequency, the structure of the antenna as shown in Fig. 5 has been scaled up by a factor of two and in other way, the operating frequency has been reduced by this factor. In 300 GHz range also the antenna shows the same directivity of 24 dBi and the gain is 23.95 dBi. The gain radiation pattern of the antenna at 297 GHz is shown in Fig. 11.

Based on this value of the gain of the antenna, the line-of-sight (LOS) distance of the terahertz communication system has been calculated with the assumptions made in [27] for binary Phase Shift Keying (BPSK), for the bit-error-rate (BER) 10^{-6}. In the present model, the channel bandwidth is 2.11 GHz at 297 GHz carrier which is shown in Fig. 12.

For 2.11 GHz bandwidth at 297 GHz carrier, the calculated value of the LOS distance is 9 m and it is quite close to the 10 m distance as indicated in the said literature. Although,

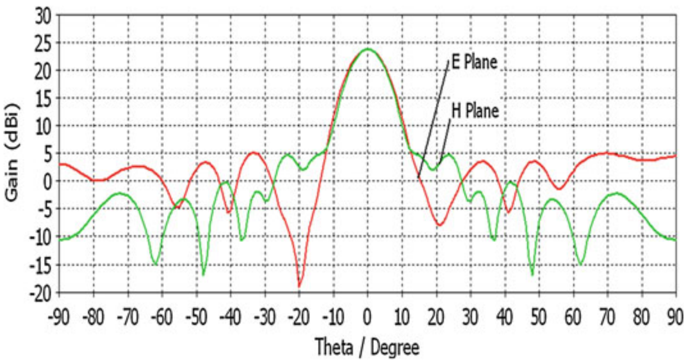

Fig. 11 Gain of the scaled down antenna at 297 GHz

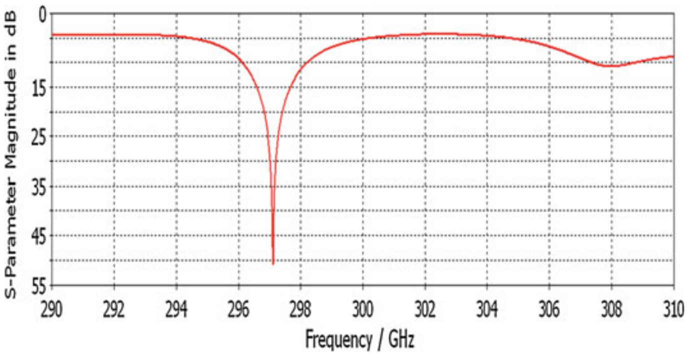

Fig. 12 S_{11} parameter of scaled down antenna

the LOS distance in the present model is close to the value of 10 m in the said literature, the gain requirement of the antenna is significantly reduced but at the cost of the bandwidth. The reduction in the gain requirement of the antenna increases the applicability of the microstrip antenna in the terahertz domain. Further, due to the reduction in the channel bandwidth, the channel noise is significantly reduced. With the reduction in the channel noise ($Pn = kTB$), channel capacity may be increased by using the advanced modulation scheme.

6 Conclusion

In this manuscript, a high directivity microstrip patch antenna at terahertz frequency has been theoretically analyzed and simulated. The simulated result shows its superiority over the various antennas presented in this band of the frequency [8–14]. The effect of the ground plane on the performance of the antenna has also been investigated. Moreover, a scaled down model of the antenna at 300 GHz has been simulated and the similar gain has been obtained. At the last, the application scenario of this kind of the antenna has been discussed and it has been noted that even with the reduced antenna gain, the communication link can be setup and with the enhancement in the modulation scheme, high data rate can be maintained.

References

1. Laskar, J., Pinel, S., Dawn, D., Sarkar, S., Perumana, B., & Sen, P. (2007). The next wireless waves is a millimeter wave. *Microwave Journal, 50*(8), 22–36.
2. Klien-Ostman, T., Pierz, K., Hein, G., Dawson, P., & Koch, M. (2004). Audio signal transmission over THz communication channel using semiconductor modulators. *Electronics Letters, 40*(2), 124–125.
3. Jastrow, C., Munter, K., Piesiewicz, R., Kurner, T., Koch, M., & Klein-Ostman, T. (2008). 300 GHz transmission system. *Electronics Letters, 44*(3), 213–214.
4. Siegel, P. H. (2002). THz technology. *IEEE Transactions on Microwave Theory and Techniques, 50*(3), 910–928.
5. Filipovic, D. F., Gearhart, S. S., & Rebeiz, G. M. (1993). Double-slot antennas on extended hemispherical and elliptical silicon dielectric lenses. *IEEE Transactions on Microwave Theory and Techniques, 41*(10), 1738–1749.
6. Jha, K. R. & Singh, G. (2009). Improved performance analysis of square patch microstrip antenna at terahertz frequency. In *Proceedings of the international conference advances in recent technologies in communication and computing (ARTCom 2009)*, India, Oct 27–28, pp. 676–679.

7. Foberg, N. M., Hu, B. B., Zhang, X.-C., & Auston, D. H. (1992). Terahertz radiation from a photoconductive antenna array. *IEEE Journal of Quantum Electronics, 28*(10), 2291–2301.
8. Jha, K. R., & Singh, G. (2010). Analysis and design of rectangular microstrip antenna on two-layer substrate materials at terahertz frequency. *Journal of Computational Electronics, 9*(2), 68–78.
9. Jha, K. R., Rao, S. V. R. K., & Singh, G. (2010) Constructive interference in Yagi-Uda type printed terahertz antenna on photonic crystal substrate. In *Proceedings of the 33rd IEEE Sarnoff conference*. Princeton, USA, Apr 12–14, pp. 1–5.
10. Han, K., Nguyen, T. K., Park, I., & Han, H. (2010). Terahertz Yagi-Uda antenna for high input resistance. *Journal of Infrared, Millimeter and Terahertz Waves, 31*(4), 441–454.
11. Singh, G. (2010). Design consideration for rectangular microstrip patch antenna on electromagnetic crystal substrate at terahertz frequency. *Infrared Physics and Technology, 53*(1), 17–22.
12. Jha, K. R., & Singh, G. (2010). Dual-band rectangular microstrip patch antenna at terahertz frequency for surveillance system. *Journal of Computational Electronics, 9*(1), 31–41.
13. Sharma, A., & Singh, G. (2009). Rectangular microstrip patch antenna design at THz frequency for short distance wireless communication systems. *Journal of Infrared, Millimeter and Terahertz Waves, 30*(1), 1–7.
14. Miao, W., Delorme, Y., Dauply, F., Lefevre, R., Lecomte, B., Feret, A., Beaudin, G., Krieg, J. M., Zhang, W., Cheng, S. H., & Shi, S. C. Investigation of a 600-GHz membrane-based twin slot antenna for HEB mixers. In: *Proceedings of 19th international symposium on space terahertz technology*, Gronigen, Netherland, Apr 28–30, pp. 563–567.
15. Liu, Z.-G., Ge, Z.-C., & Chen, X.-Y. (2009). Research progress on Fabry-Perot resonator antenna. *International Journal of Zhejiang University-Science A, 10*(4), 583–588.
16. Boutayeb, H., & Tarot, A. C. (2006). Internally excited Fabry-Perot type cavity: power normalization and directivity evaluation. *IEEE Antennas and Wireless Propagation Letters, 5*(1), 159–162.
17. Guerin, N., Enoch, S., Tayeb, G., Sabouroux, P., Vincent, P., & Legay, H. (2006). A metallic Fabry-Perot directivity antenna. *IEEE Transactions on Antennas and Wireless Propagation, 54*(1), 220–224.
18. Weily, R., Bird, T. S., & Guo, Y. J. (2008). A reconfigurable high-gain partially reflecting surface antenna. *IEEE Transactions on Antennas and Wireless Propagation, 56*(11), 3382–3390.
19. Foroozesh, A., & Shafai, L. (2009). Effects of artificial magnetic conductors in the design of low-profile high-gain planar antennas with high-permittivity dielectric superstrate. *IEEE Antennas Wireless Propagation Letters, 8*, 10–13.
20. Fu, Z., Gan, Q., Ding, Y. J., & Bartoli, F. J. (2008). From waveguiding to spatial localization of THz waves within a plasmonic metallic grating. *IEEE Journal of Selected Topics in Quantum Electronics, 14*(2), 486–490.
21. Kadoya, Y., Onuma, M., Yanagi, S., Ohkubo, T., Sato, N., & Kitagawa, J. (2008). THz wave propagation on strip lines: devices, properties and applications. *Radioengineering, 17*(2), 48–55.
22. Lin, X. Q., Cui, T. J., Fan, Y., & Liu, X. (2009). Frequency selective surface designed using electric resonant structures in terahertz frequency bands. *Journal of Electromagnetic Waves and Applications, 23*(1), 21–29.
23. Foroozesh, A., & Shafai, L. (2010). Investigation into the effects of patch-type FSS superstrate on the high-gain cavity resonance antenna design. *IEEE Transactions on Antennas and Propagation, 58*(2), 258–270.
24. Foroozesh, A. & Shafai, L. (2006). 2-D truncated periodic leaky-wave antennas with reactive impedance surface ground. In *Proceedings of the IEEE AP-S international symposium*, Albuquerque, NM, July 9–14, pp. 15–18.
25. Von Trentini, G. (1956). Partially reflecting sheet arrays. *IRE Transactions on Antennas and Propagation, 4*(4), 666–671.
26. Feresidis, A. P., & Vardaxoglou, J. C. (2001). High gain planar antenna using optimised partially reflective surfaces. *Proceedings of the Institution of Electrical Engineers, Microwaves, Antennas and Propagations, 148*(6), 345–350.
27. Piesiewiez, R., Islam, M. N., Koch, M., & Kumer, T. (2005). Towards short-range terahertz communication systems: basic consideration. *Proceedings of the 18th international conference applications electromagnetics communications, Dubrovnik, Croatia*, Oct. 12–14, pp. 1–5.

Author Biographies

Kumud Ranjan Jha passed AMIE (I) (ECE) examination from the Institution of Engineers, India, in 1999 and Master of Engineering (ECE) from Birla Institute of Technology, Ranchi, Jharkhand, India, in 2006. He received his Ph. D Degree in Electronics and Communication Engineering from Jaypee University of Information Technology, Waknaghat, Solan, Himachal Pradesh, India, in 2012. Presently, he is an Assistant Professor in the School of Electronics and Communication Engineering, Shri Mata Vaishno Devi University, Katra, Jammu and Kashmir, India. He has authored more than 30 research papers in the International Journals and Conferences of repute. His area of research is Microwave/RF passive component design and Terahertz Electronics for the future wireless communication.

G. Singh received Ph D degree in electronics engineering from the Indian Institute of Technology, Banaras Hindu University (IIT-BHU), Varanasi, India, in 2000. He was associated with Central Electronics Engineering Research Institute, Pilani, and Institute for Plasma Research, Gandhinagar, India, respectively, where he was Research Scientist. He has also worked as an Assistant Professor at Electronics and Communication Engineering Department, Nirma University of Science and Technology, Ahmedabad, India. He was a Visiting Researcher at the Seoul National University, Seoul, S. Korea. At present, he is an Associate Professor with the Department of Electronics and Communication Engineering, Jaypee University of Information Technology, Wakanaghat, Solan, India. He is the author/co-author of more than 170 scientific papers of the refereed Journal and International/National Conferences. His research interests include microwave/THz antennas and its potential applications, surface-plasmons, Electromagnetics and its applications, nanophotonics, and next generation communication systems.